

AN EXPERIMENTAL STUDY OF THE FLOWS IN AN ENERGY TRANSFER SCREW

*Susan A. Somers, Mark A. Spalding, Joseph Dooley, The Dow Chemical Company, Midland, MI
Kun Sup Hyun, Polymer Processing Institute and Chem. Eng. Dept., NJIT, Newark, NJ*

Abstract

A comparison is made between the melting, pumping, and mixing characteristics of a single-screw extruder with an Energy Transfer mixing section and a conventional screw without a mixing section. Results are given for extrusion trials, extrudate sampling, and extrusion solidification experiments performed at different screw speeds and color concentration letdown ratios.

Introduction

It is common practice to increase screw speed when attempting to increase the rate in a single-screw extruder. However, high screw speeds can transport solids close to the screw tip, which can decrease extrudate quality. Single-screw extruders equipped with specialized mixing sections can trap and melt solids to improve extrudate quality. This is due to the complex flow paths and added opportunities for shear-induced mix-melting provided by mixing sections, but the addition of mixing sections can sometimes decrease rate and increase extrudate temperature.

There have been numerous experimental studies of melting, flow, and mixing in single-screw extruders. To visualize screw performance, Maddock conducted solidification experiments, where he halted screw rotation, simultaneously cooled the barrel, and then pushed out the screw [1]. With this technique, Maddock demonstrated that melting and mixing in a conventional screw were improved by reducing the screw-channel depths, increasing the discharge pressure, or cooling the screw root. Of course, each of these adjustments had the unwanted consequence of reducing the rate. Later, he found that he could improve extrudate quality with the addition of a fluted or Maddock mixing section on the downstream end of the screw [2]. This mixer trapped and melted any solid material transported close to the screw tip and caused the extrudate temperature to increase.

More recently, Wong et al. [3] have used an extruder barrel equipped with eight windows and three pressure transducers to simultaneously observe mixing and processing performance for screws with Maddock, pineapple, pin, and barrier sections. Gale [4,5], Herridge [6], Esseghir [7], and Rios [8] have used extrudate samples and process conditions, such as power consumption, rate,

discharge temperature and pressure, to assess mixing sections. In addition, Harrah and Womer [9] have used in-line melt analysis, rates, pressure profiles, and discharge temperature homogeneity to compare several mixing sections.

In this work, we use solidification experiments, extrudate sampling, and process measurements to assess a single-screw extruder with an Energy Transfer (ET) mixing section [10]. This work builds on numerical simulations performed to study the ability of an ET section to thermally homogenize an entering melt [11,12], and it is similar to an experimental study performed for a Stratablend screw [13]. As in those previous works, we make comparisons to results for a conventional screw of similar design but without a mixing section.

This report describes results from three sets of experiments conducted for a screw with an ET section and for a conventional screw without a specialized mixing section. The ET section or screw is referred to as the mixing section or screw for the remainder of this paper. The experiments performed for each screw were:

- Extrusion flow experiments where the axial pressure, rate, extrudate temperature, and specific energy consumption were measured as a function of screw speed for extrusion of an acrylonitrile-butadiene-styrene (ABS) polymer,
- Extrusion mixing experiments where extrudate quality was assessed for a blended feed of white ABS pellets and black ABS pellets at various white to black pellet let-down ratios, and
- Extrusion solidification experiments where polymer melting mechanisms and flow patterns were frozen into place for an extruder fed a 220:1 let-down ratio of white to black ABS pellets.

Experimental Equipment and Materials

The extruder used had a 21 length-to-diameter (L/D) ratio, a 63.5 mm diameter barrel with three temperature control zones, and eleven pressure transducers distributed along its axial length [14]. The extrudate flowed from the extruder through a restrictor valve that was either fully open or partially closed. A hand-held thermocouple was used to measure extrudate temperature.

The conventional screw was square-pitched and single-flighted, with flight clearances of 0.07 mm. It had a 6-diameter feed section that was 8.89 mm deep, an 8-diameter transition section, and a 7-diameter constant-depth metering section that was 3.18 mm deep.

The mixing screw had a lead-length of 76.2 mm and a primary flight clearance of 0.08 mm. It had an 8-diameter feed section that was 10.9 mm deep, a 6-diameter transition section, and a 7-diameter mixing section. The feed and transition sections were single-flighted, and the mixing section, shown in Figure 1, was designed with two channels. The channel depths were 3.18 mm at the entrance and exit of the mixing section, and within the mixing section they oscillated between 1.45 mm and 6.35 mm. The period of these oscillations was out of phase for the two channels. In addition, the flights between the channels were undercut to 1.40 mm deep at strategic locations so that flow could occur between the channels.

The resin was an ABS polymer with a melt flow rate of 3.5g/10 min. (230°C, 3.8 kg). The white and black ABS pellets contained 2% TiO₂ and 30% pigment concentrate, respectively. The black pellets were designed for a letdown ratio of 35:1. The barrel zone temperatures were set at 200, 230, and 250°C for zones 1 (feed), 2, and 3, respectively. Screw speeds ranged from 20 to 80 rpm.

Results and Discussion

To assess pumping and melting in the screws, the steady-state axial pressures, extrudate temperatures, rates and specific energy consumption were measured as a function of screw speed. The restrictor valve was partially closed for these measurements to mimic the effect of a downstream die.

The axial pressure profiles for the two screws at a screw speed of 80 rpm are shown in Figure 2. The magnitude of the pressures were similar for both screws, increasing in the feed and transition sections and decreasing in the final turns of the metering or mixing section. One difference was that the pressure for the mixing screw reached a minimum at the entrance to the mixing section, indicating decreased resistance to flow as one of the mixing channels began to deepen. After this, the pressure increased, demonstrating the mixing section could drive flow and generate pressure. These trends also occurred at the other screw speeds.

The other processing data are summarized in Table 1. For both screws, the specific rate slightly decreased with screw speed, which is typical for flood-fed extruders. The specific rates in the mixing screw were 12 to 21% higher than the rates for the conventional screw. These differences were due to the greater lead length and slightly deeper channels of the mixing screw, and they were consistent with the specific drag flow rates and the imposed

pressure gradients in the metering channels. The calculated specific drag flow rates, due only to rotation with no imposed pressure gradients, were 0.99 and 0.89 kg/(h rpm) for the mixing and conventional screws, respectively.

The discharge temperatures for the mixing screw were 4 to 6°C lower than those for the conventional screw, showing no energy penalty for the more complex flows provided by the mixing screw. This was because the oscillating channel depths in the mixing section were designed so that viscous heating from high shear in the shallow channel regions could be balanced by low shear in the deep channel regions. Moreover, the cooler solids entrained with the molten polymer acted as a heat sink, allowing resin-to-resin heat transfer and lowering the extrudate temperature. That is, energy from the molten polymer was transferred to the cooler solids, causing the solids to melt and producing a high-quality discharge at high rates.

The specific energy inputted by the screw was 8 to 14% lower for the mixing screw. The oscillating channel depths and flight undercuts in the mixing section allowed energy from the screw to be used more effectively. Shear energy inputted to the resin in the shallow channel regions of the mixing section was readily transferred to cooler solids in the deep channel regions.

A second set of experiments was performed to characterize the mixing performance of the mixing screw. The conventional screw was included in these experiments as a baseline. The extruder was operated with a mix of white and black ABS pellets. For each screw, experiments were run using the following ratios of white to black resin: 35:1, 75:1, 100:1 and 220:1. The restrictor valve was fully opened to minimize mixing from high discharge pressures. For these experiments, the discharge pressure and rate were held constant at 8 MPa and 70 kg/h, respectively. This corresponded to a screw speed of 74 rpm for the conventional screw and 66 rpm for the mixing screw.

Figure 3 shows cross-sectional slices of the extrudate strand samples for each screw and letdown ratio. In this figure, the white spiral patterns indicate regions where little to no mixing occurred between the white and black resins. These spiral patterns were caused by the flow of the resin over the tip of the screw. Depending on the process and application, these regions could cause streaking in sheet production for extrusion operations or poor part coloration for injection molding. The unmixed white regions were most evident in the samples produced using the conventional screw. The spiral patterns were also present in the mixing screw extrudate samples. These patterns for the mixing screw, however, were considerably finer and less pronounced, indicating a much higher level of mixing.

Figure 4 shows compression moldings of the extrudate samples, which confirmed improved mixing by the mixing

screw. The compression mold at the 35:1 letdown ratio was fairly homogeneous, with only a few fine streaks of white and black. For the conventional screw, the compression moldings were heavily streaked at all letdown ratios.

The 220:1 letdown experiments were followed by solidification experiments, where screw rotation was stopped while the barrel and resin in the channels were simultaneously cooled. The combined effect caused the resin to solidify with its melting, mixing and flow patterns frozen in place. After cooling, the screw was pulled from the barrel and the helical channel of resin was unwound from the screw. The helical channel was cut lengthwise along a plane running parallel to the screw axis, revealing cross-channel slices. Figures 5 and 6 show these cross sections at axial distances of 6 to 21 diameters from the feed throat. Like the extrudate samples, the white regions indicate poor mixing because the white resin had not yet melted or the melted resin was not adequately mixed with the black concentrate. Because the black color concentrate was such an effective colorant, dark gray areas indicate where the white and black pellets melted, came in contact, and were well mixed.

As shown in Figures 5 and 6, the cross-sectional slices at axial distances less than 14 diameters were similar for both screws. For example, the slices at 6 diameters, which were at the end of the feed section, were comprised of a compacted bed of discrete pellets. At 8.5 and 8.4 diameters, the slices were in the transition section, where the pellets compacted, softened and began to melt. For the mixing screw, the compaction process had just begun at 8.4 diameters, which was only 0.4 diameters into the transition section, so discrete pellets (one black) were still visible. Still, a melt pool had begun to form near the pushing flight. This melt pool was white with black circular streaks due to the counterclockwise flow of white and black melted resin that intermingled as it made its way from the barrel to the screw root. For the conventional slice, melting was further along at 8.5 diameters, which was 2.5 diameters into the transition section. Individual pellets were no longer distinguishable and the melt pool was more mixed with finer circular striations. The slices at 12 diameters were further downstream in the transition section, so melting had further progressed. For the mixing screw, individual pellets were no longer distinguishable and the melt pool had increased in width.

At axial distances of 14 diameters and greater, the slices were different. The conventional screw had a constant depth metering section (Figure 5), and the mixing screw had a dual-channel mixing section (labeled A and B in Figure 6).

At 14.4 diameters, the mixing screw slice was divided into two channels connected by an undercut flight. This slice was only 0.4 diameters into the mixing section; so

much of the resin was still only softened, with the most of the gray molten resin segregated to the melt pool. Solid-bed breakup was observed for the mixing screw at 15 diameters, where there was striated molten resin across the entire channel, with no trace of a solid bed. It is clear that this was bed breakup, and not the completion of melting and mixing, because unmixed white resin was evident in downstream slices.

For instance, the mixing screw slice at 15.6 diameters had a segregated gray melt pool in the A-channel and much of the B-channel encompassed by white resin, similar to the slice at 14.4 diameters. For this slice, the B-channel was shallow, so the resin there experienced additional shear heating. In addition, white resin in the B-channel could flow over the flight undercut and into the adjoining and deeper A-channel where heat transfer and mixing could occur between the portions of resin that were previously in different channels. This flow caused white resin to occupy the center of the A-channel one turn downstream at 16.8 diameters. Here, the A-channel was no longer linked to its downstream B-channel neighbor by a flight undercut.

However, downstream at 17.4 diameters, the flight undercut reappeared and connected the now shallow A-channel to the upstream, and deepening, B-channel neighbor. Because the A-channel was shallow at 17.4 diameters, many of the remaining fragments of white resin were trapped, shear-heated and melted there. Furthermore, the undercut allowed resin to flow into the upstream B-channel, where resin-to-resin heat transfer and mixing occurred. The flight undercut then disappeared at 18 diameters. These trends continued at downstream positions, with the flight undercut reappearing, the B-channel becoming shallower, the A-channel becoming deeper, and the unmixed fragments of white resin becoming smaller due to periodic high shear balanced by resin-to-resin heat transfer and mixing.

By contrast, the mechanism for melting and mixing in the metering section of the conventional screw at 14 diameters and greater was limited to molten resin dragging across the barrel and collecting in the melt pool. This was quite noticeable for the slice at 16 diameters in Figure 5. In addition, there was a small amount of gray molten resin near the screw root and trailing flight for this slice.

More than likely these features were a prelude to the solid-bed breakup that occurred at 17 and 18 diameters for the conventional screw. At 17 diameters, gray molten resin encompassed the entire slice, and at 18 diameters, fragments of white resin had flowed downstream to the slice. Of course, the momentary disturbances associated with solid-bed breakup did not signify that melting was complete for the screw. In fact, the slice at 19 diameters had a gray melt pool with gray molten resin near the screw root and trailing flight, similar to the slice at 16 diameters. This was also followed by solid-bed breakup for the

conventional screw at 19.5 and 20 diameters, near the end of the screw. Of course, the solid-bed breakup was transient in nature and did not improve mixing for the conventional screw. This was demonstrated by the low mixing quality for the extrudate cross-sections and compression molds of the conventional screw.

Conclusions

This report describes an experimental study of a mixing screw with an ET mixing section. Process outputs were used to assess the screw pumping and melting performance as compared to a conventional screw of similar design but without a mixing section. Mixing performance was assessed from extrudate samples at various letdown ratios of white to black pellets and from extrusion solidification experiments.

Axial pressures, rates, discharge temperatures, and energy usage demonstrated that the mixing section did not adversely affect process performance. In fact, the screw with the mixing section generated pressure, had higher rates, had lower extrudate temperatures, and required less motor energy as compared to the conventional screw.

Extrudate samples at various colorant letdown ratios and extrusion solidification experiments, showed the mixing section improved mix-melting by allowing additional melting from high-shear in its shallow channel regions. Overheating of the resin was avoided because this high shear was brief and counter-balanced by low shear in the deep channel regions. In addition, flight undercuts in the mixing section permitted transfer of resin between the channels and resin-to-resin conductive heat transfer. The results of this design were better mix-melting, lower extrudate temperatures and reduced energy consumption for the mixing screw.

References

1. B.H. Maddock, *SPE J.*, **15**, 383 (1959).
2. B.H. Maddock, *SPE J.*, **23**, 23 (1967).
3. A. C-Y. Wong, J.C.M. Lam, T. Liu, and F. Zhu, *Adv. Polym. Tech.*, **19**, 1 (2000).
4. G.M. Gale, *SPE ANTEC Tech. Papers*, **29**, 109 (1983).
5. M. Gale, *Adv. Polym. Tech.*, **16**, 251 (1997).
6. D. Herridge and D. Krueger, *SPE ANTEC Tech. Papers*, **37**, 633 (1991).
7. M. Esseghir, C.G. Gogos, D-W. Yu, D.B. Todd, and B. David, *Adv. Polym. Tech.*, **17**, 1 (1998).
8. A.C. Rios, T.A. Osswald, M. del P. Noriega, and O.A. Estrada, *SPE ANTEC Tech. Papers*, **44**, 262 (1998).
9. G. Harrah and T. Womer, *SPE ANTEC Tech. Papers*, **44**, 267 (1998).

10. C.I. Chung, R.A. Barr, U.S. Patent 4,405,239 September 20, 1983.
11. S.A. Somers, M.A. Spalding, J. Dooley, and K.S. Hyun, *SPE ANTEC Tech. Papers*, **41**, 222 (1995).
12. T.A. Plumley, M.A. Spalding, J. Dooley, and K.S. Hyun, *SPE ANTEC Tech. Papers*, **40**, 332 (1994).
13. S.A. Somers, M.A. Spalding, K.R. Hughes, and J.D. Frankland, *SPE ANTEC Tech. Papers*, **44**, 272 (1998).
14. M.A. Spalding, J. Dooley, K.S. Hyun, and S.R. Strand, *SPE ANTEC Tech. Papers*, **39**, 1533 (1993).

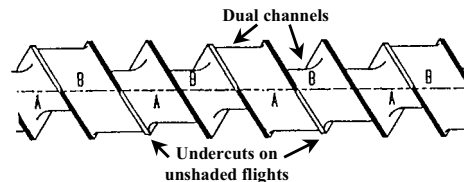


Figure 1. The mixing screw section.

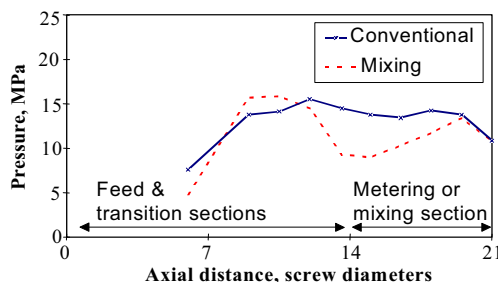


Figure 2. Pressure versus axial distance at 80 rpm.

Table 1. Process data. Conventional results in brackets.

Screw	Mixing [Conventional]			
Screw speed, rpm	20	40	60	80
Specific rate, kg/(h-rpm)	1.15 [0.95]	1.08 [0.95]	1.03 [0.92]	1.01 [0.90]
Discharge temperature, °C	253 [259]	253 [259]	254 [258]	253 [258]
Specific energy consumed, J/g	300 [350]	410 [450]	480 [520]	520 [570]

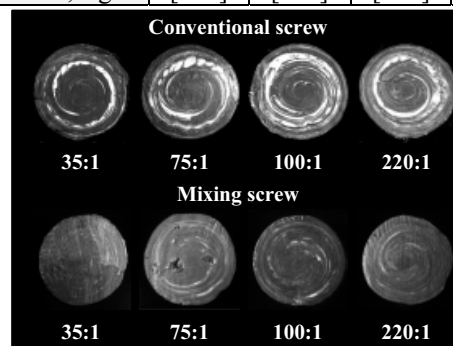


Figure 3. Cross-sectional slices of extrudate samples at 4 letdown ratios and 70 kg/h.

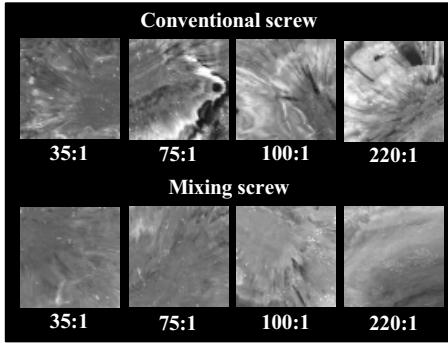


Figure 4. Compression molds of extrudate samples at 4 letdown ratios and 70 kg/h.

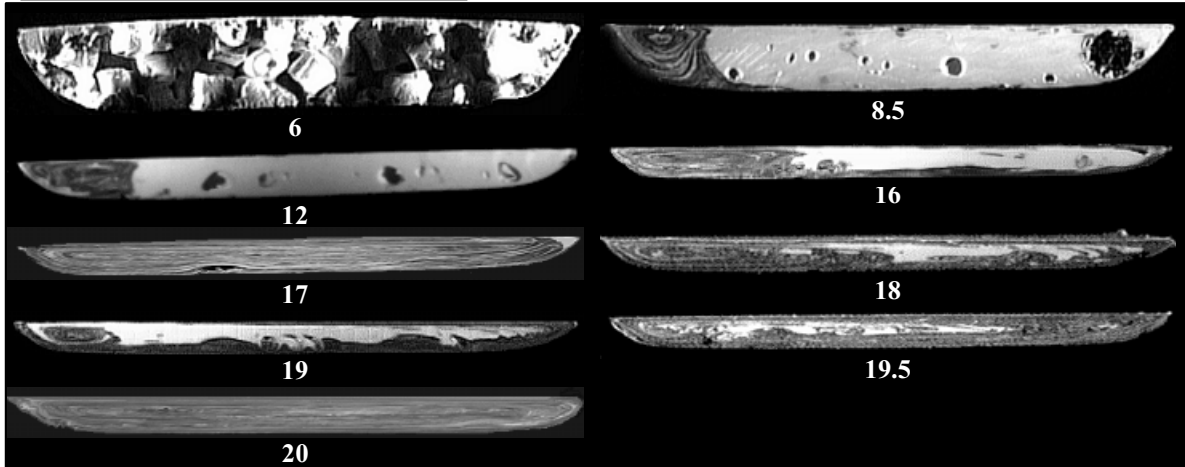


Figure 5. Cross-sectional slices for the conventional screw at a letdown ratio of 220:1. For each slice, the barrel surface is along the top, the screw root is along the bottom, and the pushing and trailing flights are along the left and right edges, respectively. Labels indicate the axial distances in screw diameters.

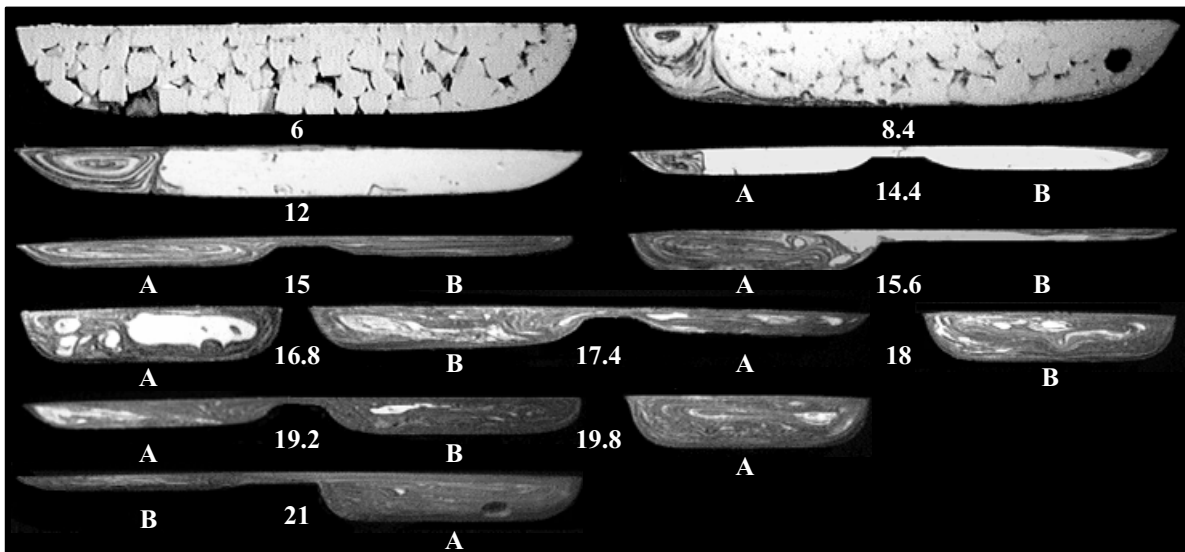


Figure 6. Cross-sectional slices for the mixing screw at a letdown ratio of 220:1. The A and B mixing channels are labeled. Other details are as in Figure 5.

Key Words: ABS, Melting, Mixing, ET, Screw Design